Electronic Supplementary Information

Point-of-care (POC) SARS-CoV-2 Antigen Detection Using Functionalized Aerosol Jet Printed Organic Electrochemical Transistor (OECT)

Jiaxin Fan,[a] Sheldon Parr,[a] Seongdae Kang[b] and Manisha Gupta[*a]

[a] Department of Electrical and Computer Engineering, University of Alberta, Edmonton, Alberta,

T6G 1H9, Canada. Email: mgupta1@ualberta.ca

[b] Department of Chemical and Materials Engineering, University of Alberta, Edmonton, Alberta,

T6G 1H9, Canada
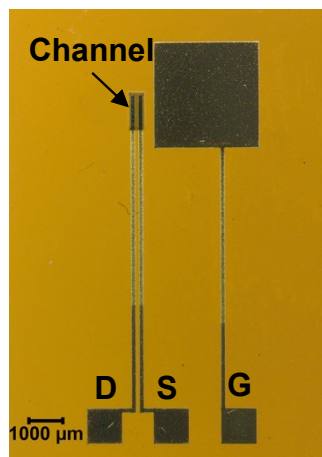
Figure S1. Microscope image of an aerosol jet printed OECT with Au source (S), drain (D), and gate (G) electrodes, PEDOT:PSS channel, and PDMS insulator. The device has a channel dimension of L = 100 μm,and W/L = 10 and gate size of 9 mm^2.
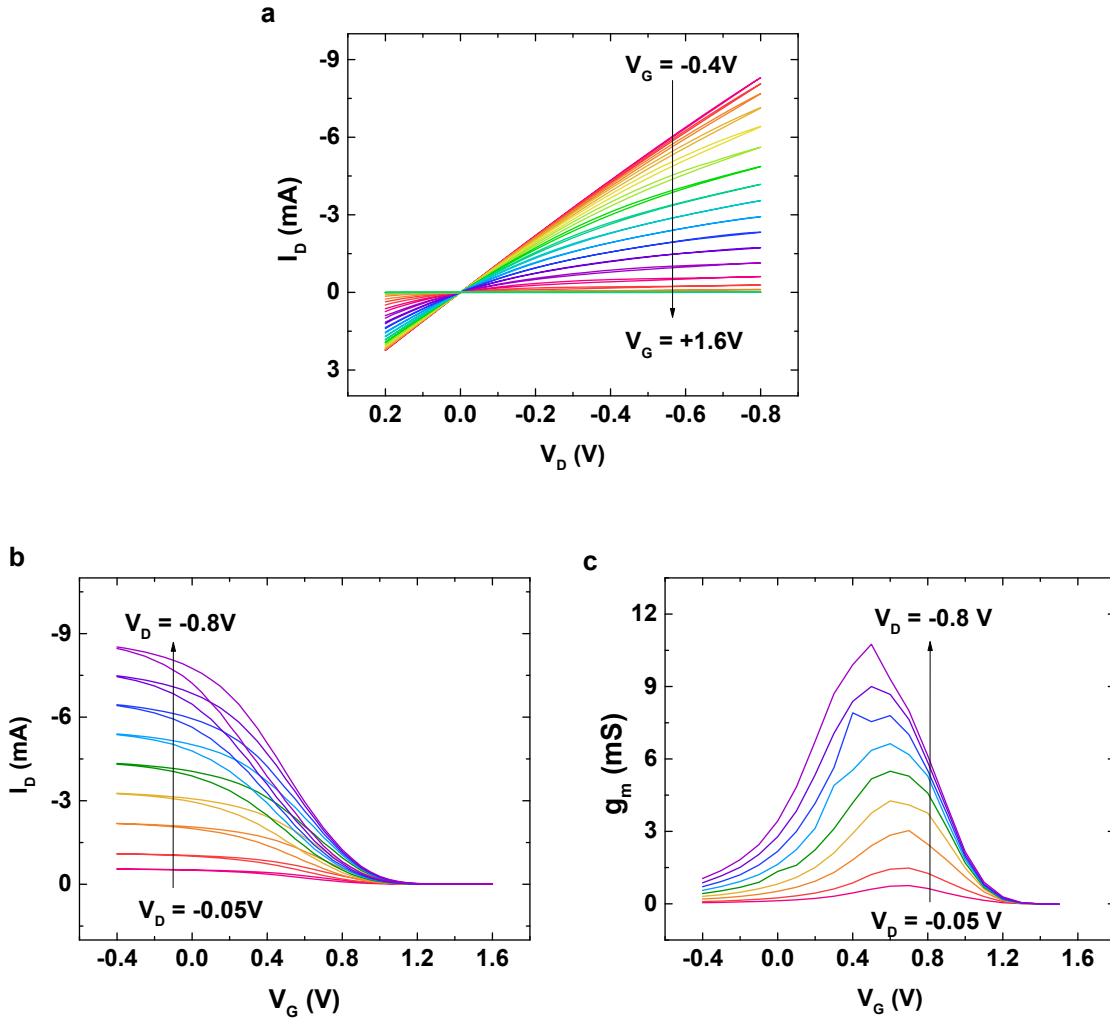
Figure S2. (a) Typical current-voltage (IV) characteristics of an unfunctionalized aerosol jet printed OECT for V_D = 0.2 to -0.8 V with V_G stepped from -0.4 to 1.6 V by 0.1 V increment. (b) Transfer characteristics for V_G = -0.4 to 1.6 V at constant V_D = 0.05, 0.1 to -0.8 V with a step size of -0.1 V. (c) The corresponding transconductance (g_m) extracted from the transfer curves measured in (b).

Functionalized Au Surface Characterization

The antibody functionalization was first verified on printed Au thin film using ATR-FTIR, fluorescence imaging, and cyclic voltammetry.

ATR-FTIR Characterization
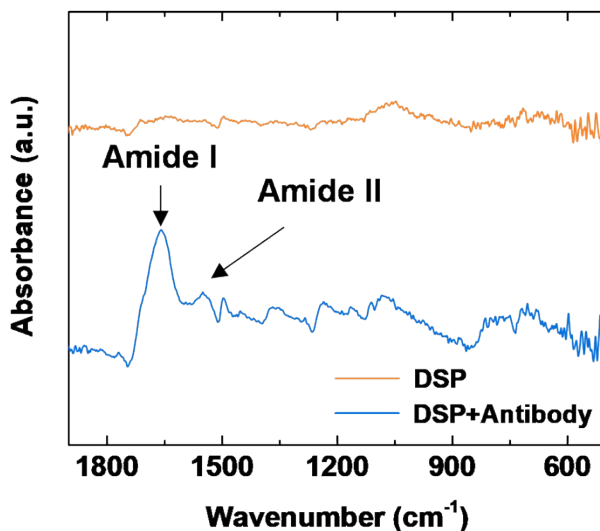
Figure S3. Infrared spectra of Au films modified with DSP only (orange) and SARS-CoV-2 antibodies via DSP (blue).

Attenuated total reflection Fourier transform infrared (ATR-FTIR) spectra were collected using a Thermo Nicolet iS50 FTIR spectrometer. The absorbance was obtained for a wavenumber range of 4000-400 cm^{-1} with a scan resolution of 4 cm^{-1} and 128 scans for each measurement. FTIR samples were prepared using printed Au films with the same procedure described for OECT functionalization. The film modified with DSP SAM was measured immediately after the

preparation. The film modified with antibody was kept in PBS buffer after functionalization, which was fully rinsed with DI water and dried with nitrogen before FTIR measurement.

Fluorescence Characterization
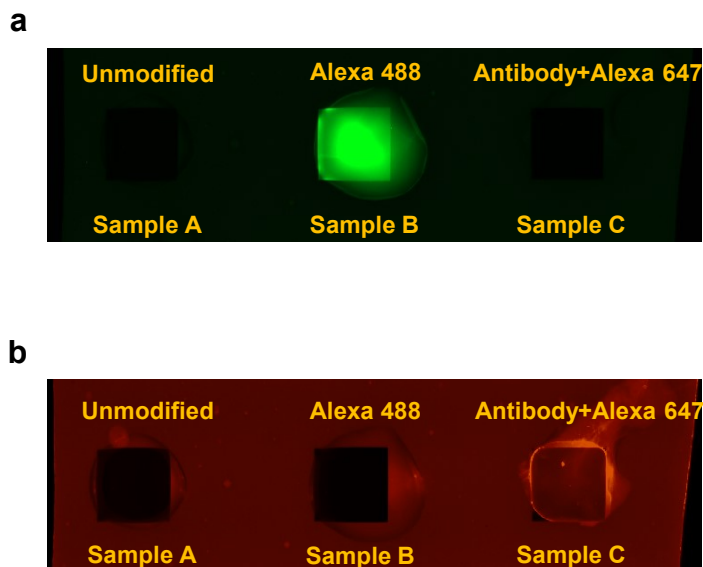
Figure S4. Fluorescence images of an unmodified Au film (Sample A), a printed Au film modified with Alexa 488 using DSP (Sample B), and a printed Au film functionalized with SARS-CoV-2 antibodies labelled with Alexa 647 (Sample C) acquired with (a) Alexa 488 (green) filter and (b) Alexa 647 (red) filter.

The fluorescence samples were prepared using the printed Au films (5 x 5 mm^2). Alexa Fluor 488 hydrazide was dissolved in 1xPBS to achieve a final concentration of 1 mM. 100 µL of SARS-CoV-2 antibody conjugated with Alexa 647 fluorophore was prepared following the quick reference provided by Thermo Fisher Scientific. The Au film functionalization was conducted using the same procedure as described for the OECT functionalization. Briefly: after modifying the two films with DSP SAM, 30 µL of 1 mM Alexa 488 hydrazide and 30 µL of Alexa 647 labeled

SARS-CoV-2 antibody solution was dispensed onto the middle and right Au films, respectively, for 2 hrs followed by cleaning with DI water and 1xPBS. Fluorescence images were taken using ChemiDoc™ MP Gel Imaging System with the samples covered with 1xPBS solution and the filters Alexa 488 and Alexa 647 for Figure S4 (a) and Figure S4 (b), respectively.

The unmodified Au film (Sample A) was used as the dark reference. Sample B, modified with DSP and Alexa 488, was for verifying the reaction of DSP with Au, which was confirmed by the green fluorescence as expected (Figure S4 (a)). Sample C, modified with DSP and SARS-CoV-2 antibodies labeled with Alexa 647, was for checking the antibody attachment to the DSP modified Au surface, which was validated by the red fluorescence (Figure S4 (b)).

Cyclic Voltammetry
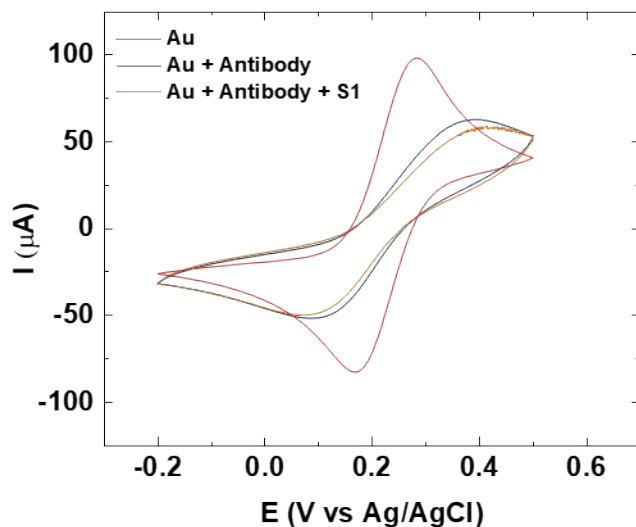
Figure S5. Cyclic voltammograms of a printed Au electrode before functionalization, after antibody immobilization, and after binding with 1 μg/mL spike S1 protein.

Cyclic voltammetry (CV) was performed using a standard three-electrode setup with 0.09 cm^2 printed Au electrode on Kapton substrate as the working electrode, a platinum counter electrode, and Ag/AgCl reference electrode (saturated with KCl). The measurements were carried out in an aqueous electrolyte containing 5 mM ferro/ferricyanide and 100 mM KCl. The CV was scanned between -0.2 and 0.5 V vs Ag/AgCl at a rate of 50 mV/s. For each sample, CV was collected for three cycles and the last cycle was used for analysis. Upon the immobilization of antibody and binding of spike S1 protein antigen, decreases in the peak current were observed due to increased electrode impedance, as expected.

OECT Device Geometry Optimization for SARS-CoV-2 Spike S1 Protein Detection

Additional details of OECT geometric optimization for SARS-CoV-2 antigen detection are described below.
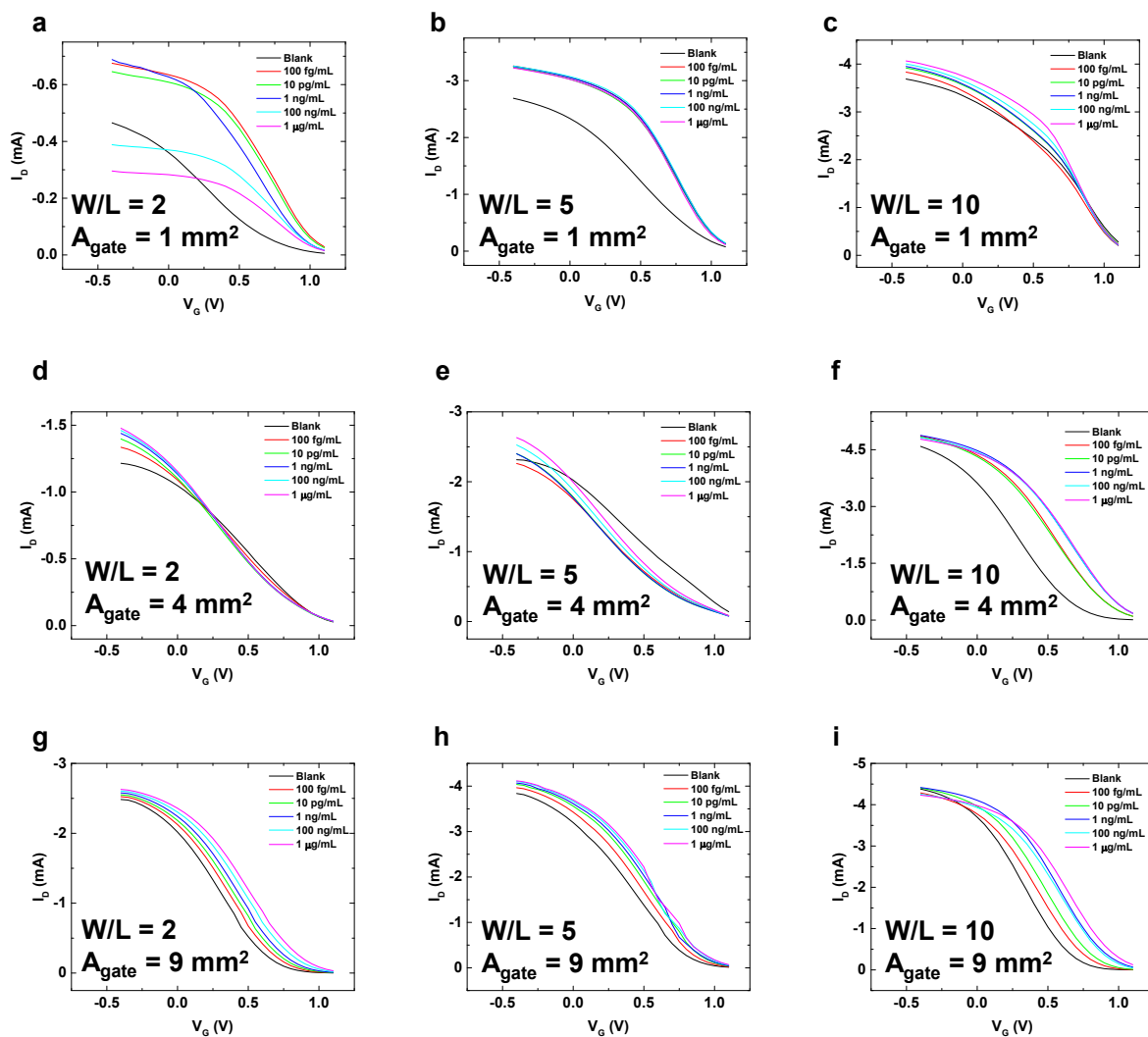
Figure S6. Transfer curves of OECTs with functionalized gate and different device dimensions (a) W/L = 2 and gate size = 1 mm², (b) W/L = 5 and gate size = 1 mm², (c) W/L = 10 and gate size = 1 mm², (d) W/L = 2 and gate size = 4 mm², (e) W/L = 5 and gate size = 4 mm², (f) W/L = 10 and gate size = 4 mm², (g) W/L = 2 and gate size = 9 mm², (h) W/L = 5 and gate size = 9 mm²,

and (i) W/L = 10 and gate size = 9 mm^2. The curves were collected after incubating with solutions of varying concentration of SARS-CoV-2 spike S1 protein.

Nine printed OECTs with the same channel length (L) of 100 μm, channel thickness of 780 nm and different channel width-to-length ratios (W/L = 1, 2, and 5) and gate sizes (A$_{gate}$ = 1, 4, and 9 mm^2) were functionalized with the SARS-CoV-2 antibody under the same conditions as described in the experimental section. The functionalized OECTs were measured with SARS-CoV-2 spike S1 protein solutions with increasing concentrations; Figure S6 shows the transfer curves collected for each device after incubation with different concentrations of SARS-CoV-2 spike S1 protein solutions. It can be observed from Figure S6 (a)-(c) that the OECTs with a gate size of 1 mm^2 did not show consistent changes. For OECTs with a gate size of 4 mm^2, only the device with W/L = 10 showed consistent shifts in the transfer curve as the S1 protein concentration increases as shown in Figure S6 (d)-(f). Figure S6 (g)-(i) shows the transfer curves for OECTs with a gate size of 9 mm^2. In this case, all three devices showed consistent shifts towards higher V$_G$ as the S1 protein concentration increased.
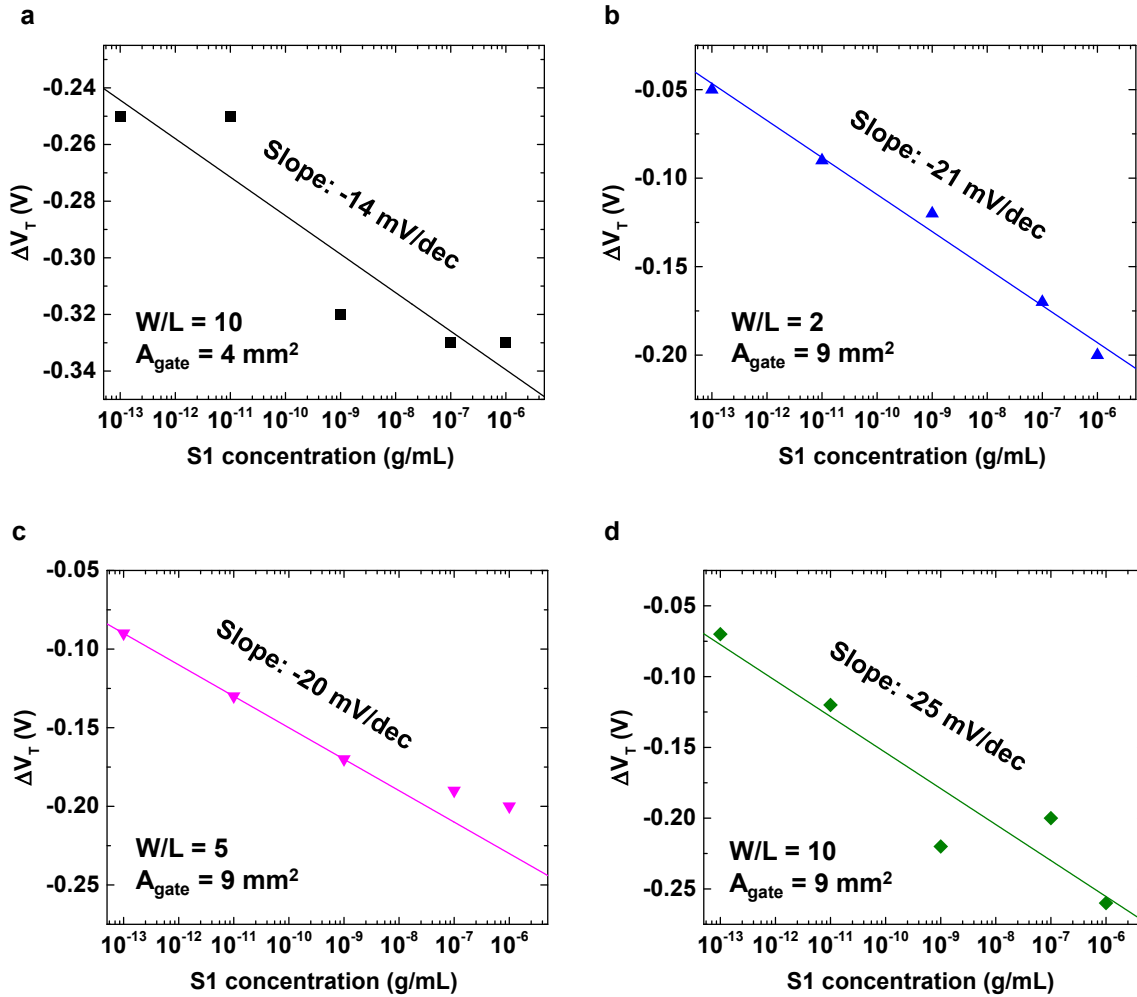
Figure S7. Semi-logarithmic plots of the average shift in threshold voltage (ΔV_T) as a function of spike protein concentration for devices with dimensions of (a) W/L = 10 and gate size = 4 mm^2, (b) W/L = 2 and gate size = 9 mm^2, (c) W/L = 5 and gate size = 9 mm^2, and (d) W/L = 10 and gate size = 9 mm^2.

The shift in the transfer curves of the four working devices was extracted as the change in the threshold voltage (ΔV_T) and plotted against the spike protein concentration, as shown in Figure S7. A logarithmic dependence of ΔV_T on the S1 protein concentration is observed, and the slope

was extracted for sensitivity analysis. Devices with a gate size of 9 mm² show higher sensitivities compared to the device with a gate size of 4 mm². For the OECTs with a gate size of 9 mm² and different W/L, it can be observed from Figure S7 (b)-(d) that the slope of the curve increases as the device W/L increases. Since transconductance is proportional to W/L, a higher W/L results in higher sensitivity.

The device dimensions, peak transconductance values, and their sensitivities for detecting S1 protein are listed in Table S1. The device transconductance is extracted from the transfer curve of the OECT and correlates with the device channel dimensions according to Equation S1:

$$g_m = \frac{\partial I_D}{\partial V_G} = \frac{Wd}{L}\mu C^*(V_T - V_G) \qquad \text{(S1)}$$

Based on the device geometry optimization, a larger gate area is required to ensure an adequate amount of antibody is immobilized onto the gate, and a higher W/L is preferred to improve the device sensitivity, due to higher transconductance. Therefore, the OECTs with a gate size of 9 mm² and W/L = 10 were selected for the SARS-CoV-2 antigen biosensor design.

Table S1. OECT gate size and channel geometry optimization for SARS-CoV-2 spike S1 protein sensing.

Gate size [mm²]	W/L	Peak transconductance (V_D= -0.4 V) [mS]	Sensitivity [mV/dec]
1	2	0.99	N/A
1	5	3.26	N/A
1	10	5.58	N/A
4	2	1.42	N/A
4	5	3.60	N/A
4	10	6.59	-14
9	2	2.91	-21
9	5	4.85	-20
9	10	6.13	-25

Customized Data Acquisition Circuit Design and Validation

Additional details of the design and validation of the data acquisition and processing circuit, developed for testing patient nasal samples, are described in this section.
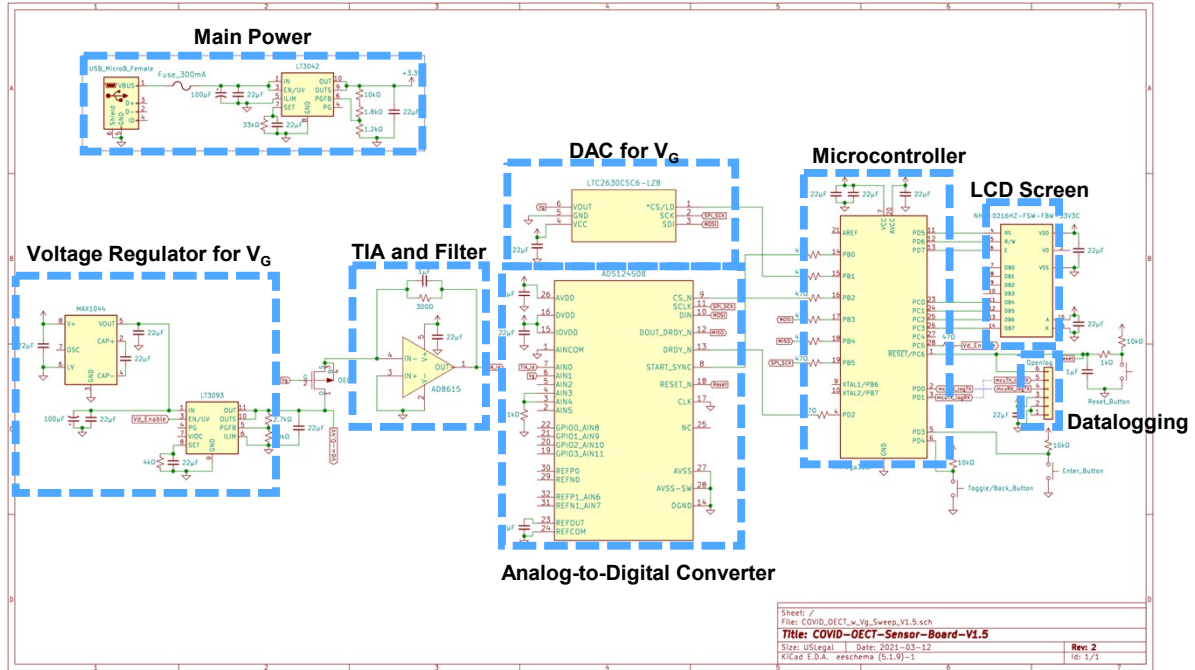
Figure S8. Schematic of the circuit board designed for measuring the OECT-based SARS-CoV-2 biosensor with a two-button user interface.

We utilized an Atmel ATmega328P microcontroller and a Texas Instruments ADS124S08 24-bit delta-sigma (Δ-Σ) analog-to-digital converter (ADC) as the core of our system. To integrate the OECT as the sensor, the V_D was biased at a constant voltage of -0.4 V using a voltage regulator, and the V_G was stepped through 0 – 1.121 V using an 8-bit digital to analog converter (DAC) with

a step size of approximately 49 mV. As the OECT sensor relies on the change of I_D for SARS-CoV-2 detection, a transimpedance amplifier (TIA) was used to convert the current signal into a voltage, V_{Id}. The feedback resistor (R_{gain}) was selected based on the OECT I_D magnitude measured using the Keithley source meter to ensure that the converted voltage would be within the input voltage range of the 24-bit Δ-Σ ADC and finely resolved for the threshold voltage extraction. Both V_G and V_{Id} were measured by the ADC for each step of V_G, and the raw ADC data was then transferred by the central microcontroller to an Openlog datalogger and saved on a microSD card. The TIA and ADC were characterized in the lab using a Keithley source meter to validate their output response. The calibration curves for the TIA and ADC demonstrated excellent linearity with a coefficient of determination $R^2 = 1$ as shown in Figure S9 (a)-(b).
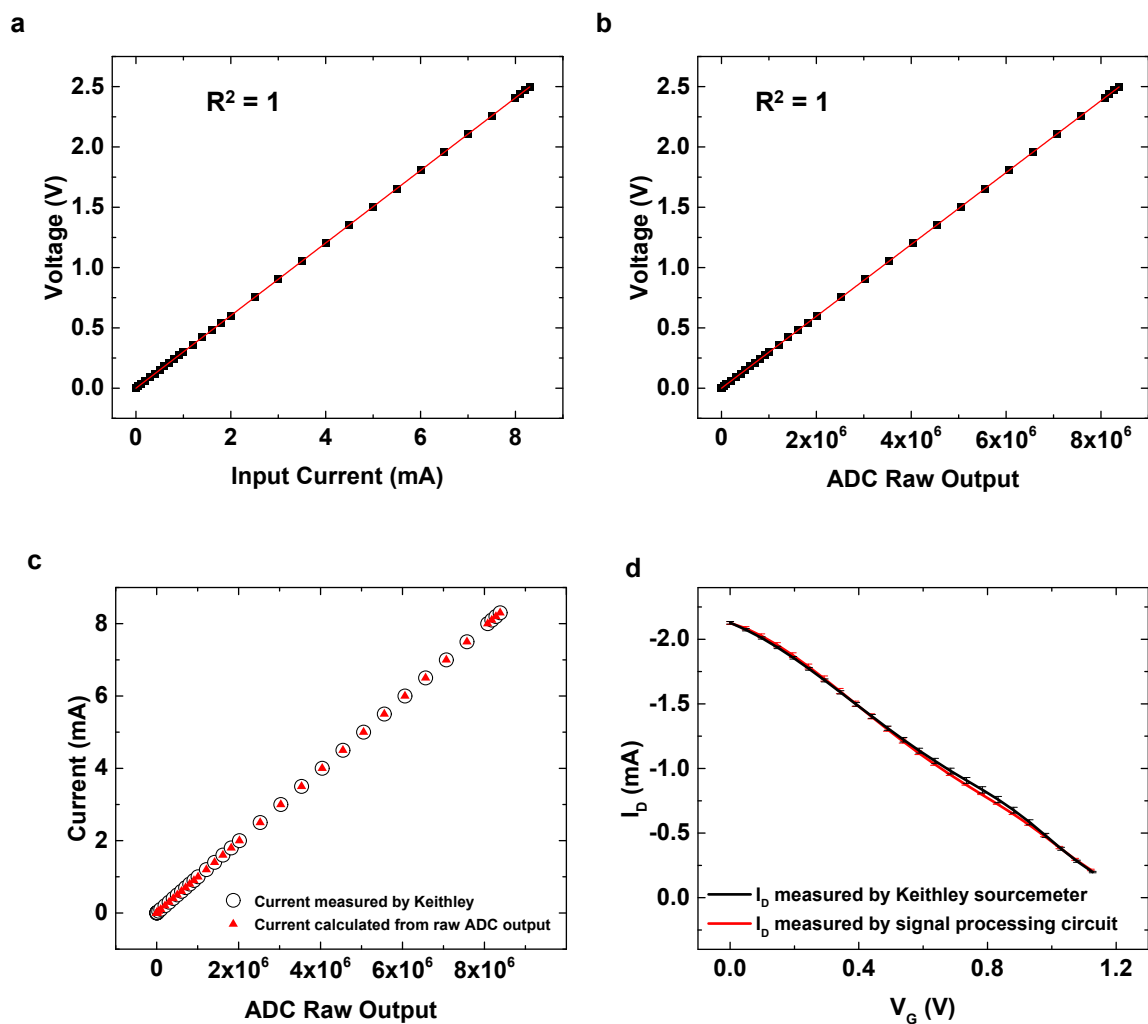
Figure S9. (a) Calibration curve of the TIA obtained by sourcing the input current and measuring the output voltage using a Keithley sourcemeter. The linear fit has a slope of 301 Ω which matches the value of the feedback resistor, R^2= 1, and a small offset voltage of -31.6 µV. (b) Calibration curve of the 24-bit Δ-Σ ADC collected by using a Keithley sourcemeter to source the input current and comparing the output of ADC raw data and the ADC pin voltage measured by Keithley. A linear correlation between the two sets of values with R^2=1 and a small ADC offset voltage of -115 µV is observed. (c) Scatter plots showing the input current sourced by Keithley and the

calculated current from the ADC output coincide with each other with <1% variation. (d) Comparison of the transfer curve obtained by the signal processing circuit to the one obtained by Keithley sourcemeter. The plots are the average of four measurements collected from each system, and the error bars represent the standard deviation. The average discrepancy of all points obtained through the two methods is 2%.

The circuit performance was verified using the Keithley sourcemeter. The current values calculated from the raw ADC data match the input current values measured with the sourcemeter (Figure S9 (c)). The circuit performance was further verified by comparing the measurements of the same OECT acquired by the two systems, which nearly coincide with only 2% average discrepancy (Figure S9 (d)). The SARS-CoV-2 spike protein sensing results measured by the circuit (Figure S10) are similar to those obtained by the sourcemeter. Therefore, the circuit has sufficient precision for the desired purposes.
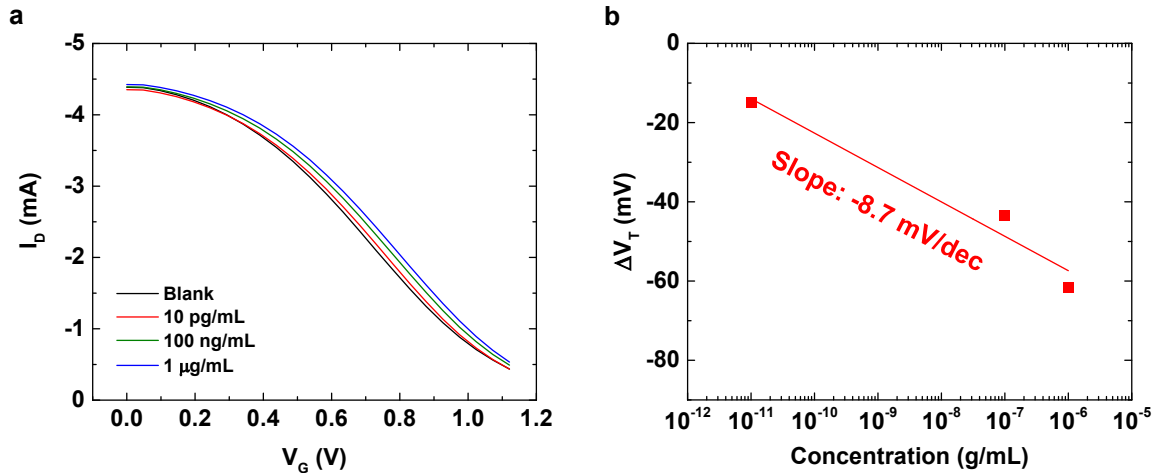
Figure S10. (a) Circuit collected transfer characteristics of a functionalized OECT measured after being incubated in increasing concentration of SARS-CoV-2 spike S1 protein solution. (b) Semi-logarithmic plot of ΔV_T as a function of spike protein concentration extracted from the transfer curves collected using the data processing circuit.
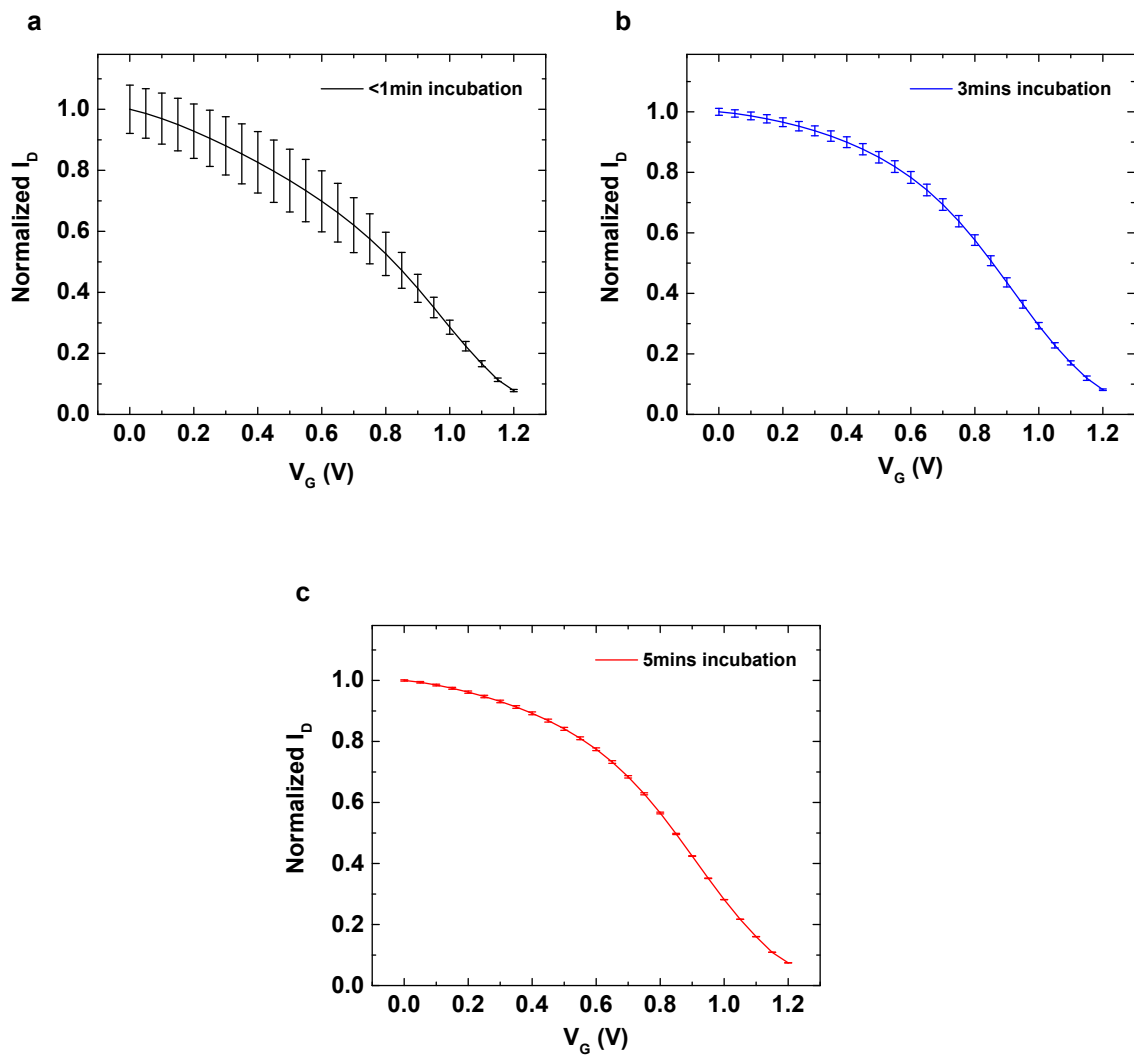
Figure S11. Blank UTM testing using aerosol jet printed OECT. Normalized I_D vs V_G curve averaged over three consecutive measurements with (a) less than 1 min incubation time, (b) 3 mins incubation time, and (c) 5 mins incubation time between each measurement. The error bars represent the standard deviation.

Table S2. COVID-19 results of patient samples acquired by PCR and OECT-based biosensor.

Biosensor ID	PCR Result	Ct [cycles]	ΔV_T [mV]	OECT Result
D1	Negative	-	-3.88	Negative
D3	Negative	-	-17.60	False Positive
C2	Negative	-	-4.55	Negative
E1	Negative	-	-8.15	Negative
E3	Negative	-	-27.24	Defective
D2	Positive	23.46	-15.50	Positive
C1	Positive	26.23	-1.11	Defective
B3	Positive	26.87	-16.09	Positive
E2	Positive	36	-14.26	Positive
C3	Positive	14.67	-20.76	Positive

Table S3. Threshold voltage values of the OECT devices used for real COVID-19 patient sample testing before functionalization. The values are extracted from transfer curves measured in PBS for three consecutive measurements. The standard deviation (σ) for the threshold voltage values is also listed.

Biosensor ID	V_T - 1st [V]	V_T - 2nd [V]	V_T - 3rd [V]	Average V_T [V]	σ [V]
C1	1.02962	1.02975	1.03207	1.03048	0.00138
D3	1.09482	1.09144	1.08873	1.09167	0.00305
E3	1.11200	1.11009	1.10961	1.11057	0.00126
C2	1.07421	1.07424	1.07175	1.07340	0.00143
C3	1.19789	1.18459	1.17843	1.18697	0.00995
D1	1.04052	1.03639	1.03530	1.03741	0.00275
D2	1.08915	1.08197	1.07777	1.08296	0.00575
B3	1.19965	1.19416	1.19130	1.19504	0.00425
E1	1.04623	1.04663	1.04456	1.04581	0.00110
E2	1.14039	1.13386	1.12928	1.13451	0.00559
Average σ [V]	-	-	-	-	0.00365
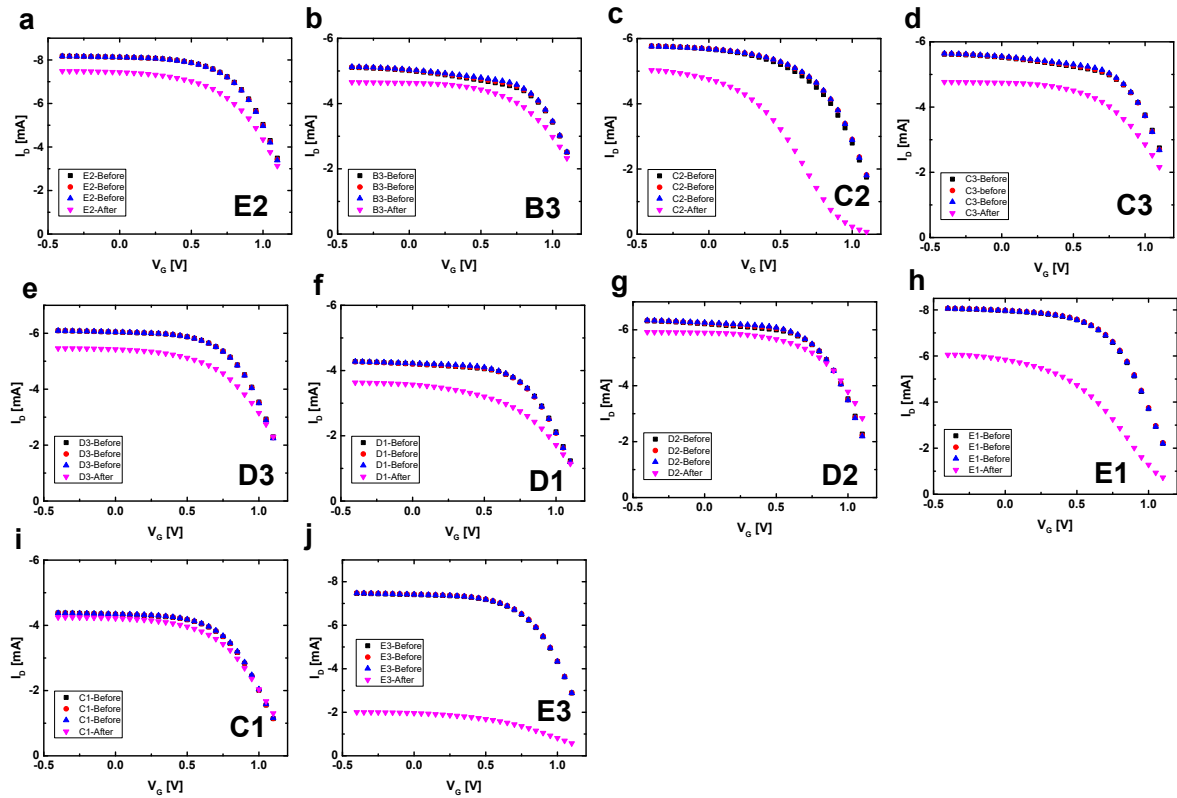
Figure S12. Transfer curves of devices used for patient sample testing measured in 1xPBS before and after functionalizing the Au gate with SARS-CoV-2 antibody. (a)-(h) Devices that were successfully functionalized. (i)-(j) Defective devices: note the negligible shift in curves before and after functionalization in (i) and the considerably larger than typical shift in (j) compared to the rest of the device set.

Table S4. List of components and their costs in the COVID-19 diagnostic tool based on the research expenses

Components/Description	Estimated cost in CAD
Components for the circuit	$172.98
PCB boards (including data processing circuit board and the ZIF connector breakout board)	$3.50
3D printed circuit enclosure	$3.00
Total cost for the circuit board	**$179.48**
Materials for printing one sensor	$2.89
Materials for functionalizing one sensor	$15.44
Total cost per sensor	**$18.33**

The estimated fabrication costs (circuit: $179.48, one biosensor: $18.30) of our COVID-19 diagnostic tool are listed in Table S4. The relatively high expense is mainly due to the high unit cost of purchasing low SARS-CoV-2 antibody amounts, which will be lower for bulk orders. We anticipate reducing the overall manufacturing cost around 20- to 100-fold for mass production.